

Secondary lymphoid tissue chemokine (SLC/CCL21)/CCR7 signaling regulates fibrocytes in renal fibrosis

Norihiko Sakai*, Takashi Wada*^{†‡}, Hitoshi Yokoyama[§], Martin Lipp[¶], Satoshi Ueha^{||}, Kouji Matsushima^{||}, and Shuichi Kaneko*

*Disease Control and Homeostasis, Kanazawa University Graduate School of Medical Science, and [†]Division of Blood Purification, Kanazawa University, 13-1 Takara-machi, Kanazawa 920-8641, Japan; [§]Division of Nephrology, Kanazawa Medical University, Kahoku, Ishikawa 920-0293, Japan; ^{||}Department of Molecular Preventive Medicine, Graduate School of Medicine, University of Tokyo, Tokyo 113-033, Japan; and [¶]Molecular Tumorigenetics and Immunogenetics, Max Delbrück Center for Molecular Medicine, 13092 Berlin, Germany

Edited by Richard Bucala, Yale University School of Medicine, New Haven, CT, and accepted by the Editorial Board July 24, 2006 (received for review January 3, 2006)

Fibrocytes are a distinct population of bloodborne cells that share markers of leukocytes as well as mesenchymal cells. We hypothesized that CCR7-positive fibrocytes migrate into the kidney in response to secondary lymphoid tissue chemokine (SLC/CCL21) and contribute to renal fibrosis. To investigate this hypothesis, renal fibrosis was induced by unilateral ureteral obstruction in mice. A considerable number of fibrocytes dual-positive for CD45 and type I collagen (Coll) or CD34 and Coll infiltrated the interstitium, reaching a peak on day 7. Most fibrocytes were positive for CCR7, and CCL21/CCR7 blockade reduced the number of infiltrating fibrocytes. CCL21 and MECA79 dual-positive vessels were also detected in the interstitium. The blockade of CCL21/CCR7 signaling by anti-CCL21 antibodies reduced renal fibrosis, which was confirmed by a decrease in fibrosis in CCR7-null mice with concomitant reduction in renal transcripts of pro α 1 chain of Coll and TGF- β 1. The number of F4/80-positive macrophages decreased along with renal transcripts of monocyte chemoattractant protein 1 (MCP-1/CCL2) after the blockade of CCL21/CCR7 signaling. These findings suggest that CCR7-positive fibrocytes infiltrate the kidney via CCL21-positive vessels, thereby contributing to the pathogenesis of renal fibrosis. Thus, the CCL21/CCR7 signaling of fibrocytes may provide therapeutic targets for combating renal fibrosis.

kidney | CD45

Fibrosis is a hallmark of progressive organ diseases, resulting in organ failure. Despite varied etiologies, renal diseases progress to end-stage renal failure characterized by glomerulosclerosis and interstitial fibrosis (1, 2). In addition, renal fibrosis determines the prognosis of renal diseases independent of their etiologies (3, 4). The histological picture of renal fibrosis is characterized by tubular atrophy and dilation, interstitial leukocyte infiltration, accumulation of fibroblasts, and increased interstitial matrix deposition (5). Currently, resident fibroblasts, epithelial–mesenchymal transition (EMT)-derived fibroblasts/myofibroblasts, and monocytes/macrophages are thought to be participants in the pathogenesis of renal fibrosis (6–9). However, the precise pathogenic mechanisms of renal fibrosis remain to be determined.

A circulating bone marrow-derived population of fibroblast-like cells (termed fibrocytes) was first identified a decade ago (10). Fibrocytes comprise a minor fraction of the circulating pool of leukocytes (<1%) and share the markers of leukocytes (e.g., CD45 and CD34) as well as mesenchymal cells [e.g., type I collagen (Coll) and fibronectin] (11, 12). Fibrocytes are present in experimental fibrosis associated with conditions such as pulmonary fibrosis, bronchial asthma, and skin wounds (13–15). Furthermore, fibrocytes are detected in human fibrosing diseases including nephrogenic fibrosing dermopathy and burns (16, 17). CD34-positive spindle cells are also reported to be

present in the interstitium in patients with glomerulonephritis (18). In addition, fibrocytes express chemokine receptors such as CCR7, CXCR4, and CCR2 (12, 13). Recent studies demonstrated that chemokine receptors on fibrocytes are involved in the recruitment of circulating fibrocytes to sites of fibrosis (12, 13). However, the roles of fibrocytes in the pathogenesis of renal fibrosis and their trafficking into diseased kidneys have not been fully investigated.

A ligand for CCR7, secondary lymphoid tissue chemokine (SLC/CCL21), is a member of the CC chemokine family, the first two cysteine residues of which are adjacent to each other. CCL21 contains six cysteines and is a potent chemoattractant for T cells, B cells, and dendritic cells (19–21). In addition, CCL21 also acts as a chemotactic stimulus for fibrocytes (15). In humans as well as in mice, CCL21 is constitutively abundant in lymphoid tissues, particularly in the lymph nodes and spleen. It is of note that CCL21 is also expressed at lower levels in some nonlymphoid tissues, including the lung (20). CCL21 expression has been shown to be localized in high endothelial venules (HEVs) in lymph nodes under physiological conditions (20) as well as in nonlymphoid tissues under inflammatory conditions (22).

These findings prompted us to examine whether the contribution of fibrocytes to renal fibrosis depends on CCL21/CCR7 signaling. To address this issue, we evaluated renal fibrosis induced by unilateral ureteral obstruction (UUO), a well known renal fibrosis model (23, 24), in mice treated with specific neutralizing anti-CCL21 antibodies and in CCR7-null mice. We report here that fibrocytes were pivotally involved in the pathogenesis of renal fibrosis and that blockade of CCL21/CCR7 signaling represented a beneficial therapeutic approach to progressive fibrosis of the kidney in this mouse model.

Results

Effect of Inhibition of CCL21/CCR7 Signaling on Renal Fibrosis and Coll Expression. To determine the impact of CCL21/CCR7 signaling on progressive renal interstitial injury, interstitial fibrotic areas expressed as blue on Mallory–Azan-stained histological samples were examined by computer analysis. In wild-type mice, ureteral ligation caused progressive renal fibrosis in obstructed kidneys (Fig. 1*a* and *f*). In contrast, the mean interstitial fibrosis, expressed as percentage per square millimeter, was reduced in mice treated with anti-CCL21 antibodies and in CCR7-null mice compared with that

Conflict of interest statement: No conflicts declared.

This paper was submitted directly (Track II) to the PNAS office. R.B. is a guest editor invited by the Editorial Board.

Abbreviations: HEV, high endothelial venule; UUO, unilateral ureteral obstruction; EMT, epithelial–mesenchymal transition; Coll, type I collagen.

[†]To whom correspondence should be addressed. E-mail: twada@m-kanazawa.jp.

© 2006 by The National Academy of Sciences of the USA

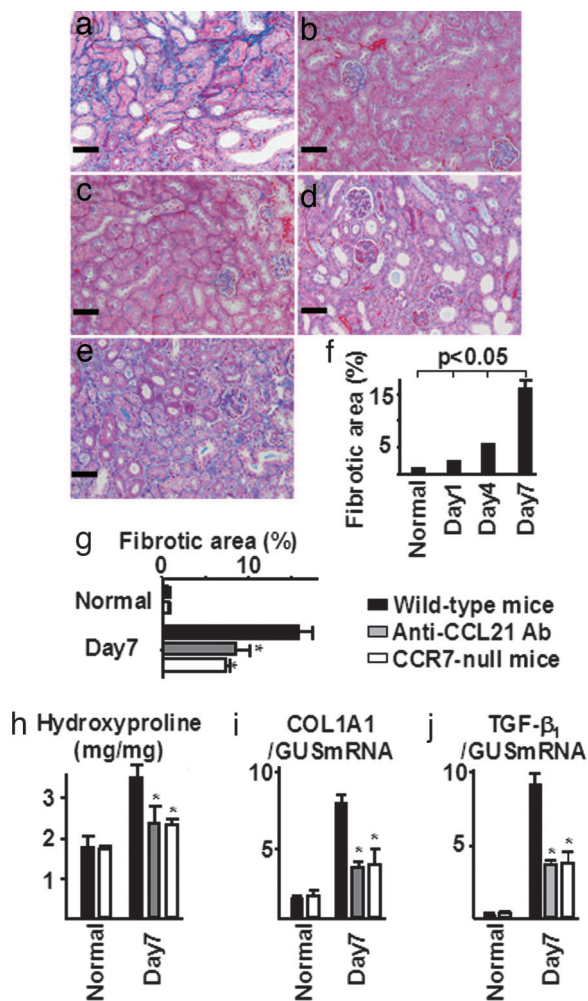


Fig. 1. Inhibition of CCL21/CCR7 signaling reduced renal fibrosis. In wild-type mice, ureteral ligation caused progressive renal fibrosis in obstructed kidneys (a and f) compared with that in normal kidneys (b) and in contralateral kidneys (c). In contrast, the mean interstitial fibrosis was reduced in obstructed kidneys treated with anti-CCL21 antibodies (d) and in CCR7-null mice (e) compared with that in UUO-treated wild-type mice 7 days after UUO (g). Total tissue collagen content (hydroxyproline) was markedly reduced in mice treated with anti-CCL21 antibodies and in CCR7-null mice compared with that in UUO-treated wild-type mice 7 days after UUO (h). The up-regulated mRNA expression of Coll as well as TGF- β_1 in diseased kidneys was reduced by CCL21/CCR7 signaling blockade (i and j). Mallory–Azán staining was done at an original magnification of $\times 200$. Values are the mean \pm SEM. *, $P < 0.05$ compared with wild-type mice on day 7. (Scale bars: 50 μ m.)

in wild-type mice 7 days after UUO (Fig. 1 d, e, and g). In addition, the amount of hydroxyproline was evaluated for a more quantitative measurement to determine tissue collagen content. Similar to the computer-assisted measurement of renal fibrotic area, total tissue collagen content was significantly reduced in mice treated with anti-CCL21 antibodies and in CCR7-null mice (Fig. 1h). Furthermore, ureteral ligation enhanced the pro $\alpha 1$ chain of Coll (COL1A1) mRNA expression in wild-type mice, which was significantly reduced by blockade of CCL21/CCR7 signaling (Fig. 1i). Seven days after ureteral ligation, transcripts of TGF- β_1 , which is a profibrotic molecule, were up-regulated in wild-type mice, whereas the levels were reduced in mice treated with anti-CCL21 antibodies as well as in CCR7-null mice (Fig. 1j). Thus, CCL21/CCR7 signaling appears to play a role in the pathogenesis of renal fibrosis.

Fibrocytes Infiltrated the Kidney After Ureteral Ligation. One of the unique characteristics of fibrocytes is the simultaneous expression

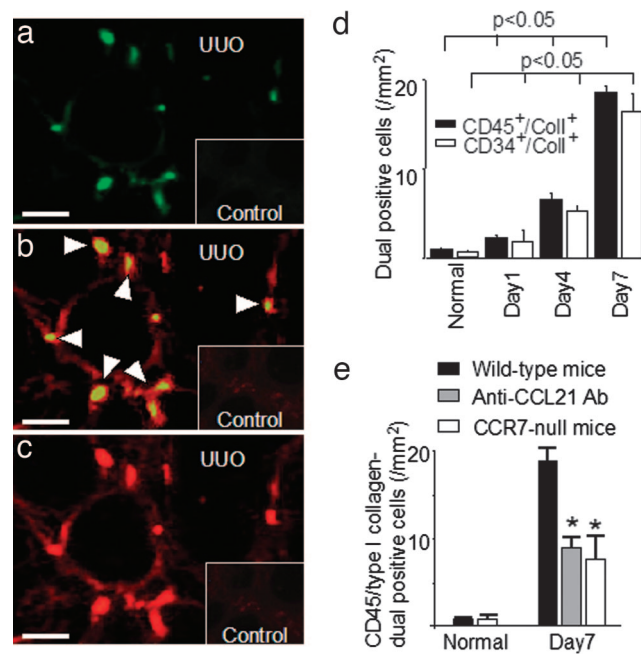


Fig. 2. Fibrocytes infiltrated the kidney after ureteral ligation. In wild-type mice, CD45⁺/Coll⁺ fibrocytes infiltrated the interstitium, especially the corticomedullary regions after ureteral ligation. (a) CD45. (b) Merge. (c) Coll. Arrowheads indicate CD45⁺/Coll⁺ fibrocytes. The number of infiltrating fibrocytes (CD45⁺/Coll⁺ and CD34⁺/Coll⁺) increased with the progression of fibrosis after ureteral ligation, reaching a peak on day 7 (d). In contrast, the number of infiltrating fibrocytes (CD45⁺/Coll⁺) was reduced in mice treated with anti-CCL21 antibodies (8.8 \pm 1.8 per square millimeter; $n = 7$) and in CCR7-null mice (7.5 \pm 1.4 per square millimeter; $n = 7$) compared with that in wild-type mice (19.2 \pm 2.5 per square millimeter; $n = 7$) 7 days after ureteral ligation (e). Values are the mean \pm SEM. UUO, UUO-treated wild-type mice; Control, untreated wild-type mice. *, $P < 0.05$ compared with wild-type mice on day 7. (Scale bars: 50 μ m.)

of both leukocyte markers, such as CD45 and CD34, and Coll (12). Therefore, these cells are identified in tissue samples by double immunohistochemistry using specific antibodies against CD45 and Coll. In wild-type mice with ureteral ligation, CD45 and Coll dual-positive fibrocytes (CD45⁺/Coll⁺) infiltrated the interstitium, especially the corticomedullary regions (Fig. 2 a–c). The number of infiltrating fibrocytes increased with the progression of fibrosis after ureteral ligation, reaching a peak on day 7 (19.2 \pm 2.5 per square millimeter; $n = 7$) (Fig. 2d). To further verify the existence of fibrocytes, dual immunostainings of CD34 and Coll were also performed. The infiltration of CD34 and Coll dual-positive fibrocytes was observed in the interstitium and correlated with disease progression as determined by CD45 and Coll dual immunostainings (Fig. 2d). In addition, dual-labeling was performed by immunofluorescence immunohistochemistry to determine the presence of CCR7-expressing fibrocytes. Expressions of both CCR7 and Coll were assessed, because CCR7-positive T cells, B cells, and dendritic cells are not capable of producing Coll. CCR7-expressing fibrocytes positive for both CCR7 and Coll (CCR7⁺/Coll⁺) were detected in diseased kidneys 7 days after UUO in wild-type mice (Fig. 3 a–c). Furthermore, flow cytometry analyses of renal cells isolated from normal kidneys, obstructed kidneys, and contralateral kidneys 7 days after UUO were performed to determine the characteristics of infiltrating fibrocytes. In wild-type mice, the ratio of CCR7⁺/Coll⁺ cells in obstructed kidneys was increased to 7.9% of the total isolated renal cells compared with that in normal kidneys (0.25%) and contralateral kidneys (0.21%) (Fig. 3d). Of these CCR7-expressing fibrocytes in obstructed kidneys, 66.5% of cells were CXCR4⁺/CCR2⁺, 16.8% of cells were CXCR4⁺/CCR2⁻, 4.3% of

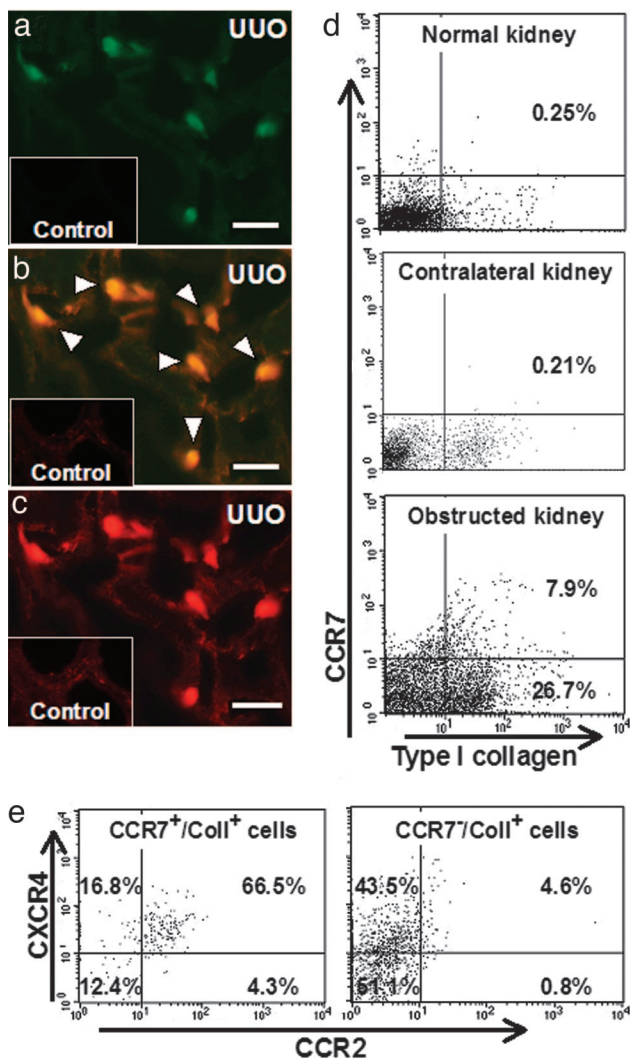


Fig. 3. Infiltrating fibrocytes were positive for CCR7 as well as CXCR4 and CCR2. Immunofluorescence immunohistochemistry and flow cytometry were performed to determine the presence of CCR7 on infiltrating fibrocytes by detecting CCR7 and Coll. Dual-positive cells for CCR7 and Coll were detected in diseased kidneys 7 days after ureteral ligation in wild-type mice in immunohistochemical studies. (a) CCR7. (b) Merge. (c) Coll. Arrowheads indicate CCR7⁺/Coll⁺ fibrocytes. In wild-type mice, flow cytometry analyses demonstrated that the proportion of CCR7⁺/Coll⁺ cells in obstructed kidneys was increased to 7.9% of the total isolated renal cells compared with that in normal kidneys (0.25%) and contralateral kidneys (0.21%) (d). Of these CCR7-expressing fibrocytes in obstructed kidneys, 66.5% were CXCR4⁺/CCR2⁺, 16.8% were CXCR4⁺/CCR2⁻, 4.3% were CXCR4⁻/CCR2⁺, and 12.4% were CXCR4⁻/CCR2⁻ (e Left). In addition, the percentages of CCR7-negative collagen-producing cells (CCR7⁻/Coll⁺) rose to 26.7% of the isolated renal cells in obstructed kidneys (d). Of these CCR7⁻/Coll⁺ cells, 48.9% (13.0% of total isolated cells) were thought to be CCR2⁻ and/or CXCR4-positive fibrocytes (CCR7-nonexpressing fibrocytes) (e Right). UUO, UUO-treated wild-type mice; Control, untreated wild-type mice. (Scale bars: 50 μ m.)

cells were CXCR4⁻/CCR2⁺, and 12.4% of cells were CXCR4⁻/CCR2⁻ (Fig. 3e). In addition, the percentage of CCR7-negative collagen-producing cells (CCR7⁻/Coll⁺) increased to 26.7% of the total isolated renal cells from obstructed kidneys (Fig. 3d). Furthermore, 48.9% of these CCR7⁻/Coll⁺ cells (13.0% of total isolated cells) were thought to be CCR2⁻ and/or CXCR4-expressing fibrocytes (CCR7-nonexpressing fibrocytes) (Fig. 3e). As a result, 37.8% of infiltrating fibrocytes expressed CCR7 (number of CCR7⁺/Coll⁺ divided by the number of CCR7⁺ or CXCR4⁺ or CCR2⁺/Coll⁺).

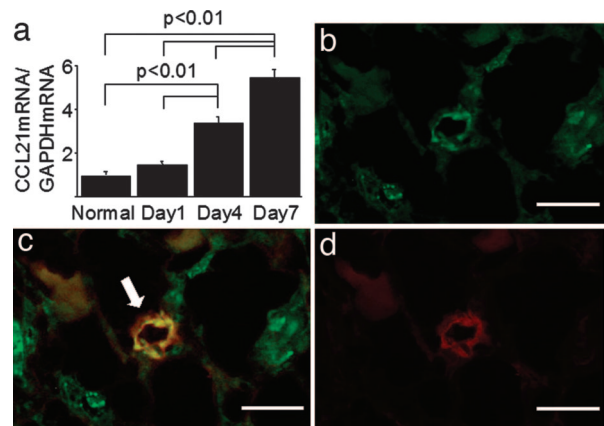


Fig. 4. CCL21-positive HEV-like vessels were detected in fibrotic kidney. The expression of CCL21 mRNA in diseased kidneys was up-regulated with progression of fibrosis in wild-type mice (a). Furthermore, the colocalization of CCL21 protein with MECA79-positive vessels was detected in the corticomedullary junction on day 7. (b) CCL21. (c) Merge. (d) MECA79. Arrow, CCL21 and MECA79 dual-positive vessel. Values are the mean \pm SEM. (Scale bars: 50 μ m.)

CCL21/CCR7-Dependent Fibrocyte Infiltration in the Kidney. To elucidate the role of CCL21/CCR7 interaction in the infiltration of fibrocytes into the kidney, anti-CCL21 antibody-treated mice and CCR7-null mice were used. The number of infiltrating fibrocytes (CD45⁺/Coll⁺) was reduced both in mice treated with anti-CCL21 antibodies (8.8 ± 1.8 per square millimeter; $n = 7$) and in CCR7-null mice (7.5 ± 1.4 per square millimeter; $n = 7$) compared with that in wild-type mice (19.2 ± 2.5 per square millimeter; $n = 7$) 7 days after UUO (Fig. 2e). It was further noted that the number of CCR7⁺/Coll⁺ was also decreased in mice treated with anti-CCL21 antibodies (4.8 ± 1.8 per square millimeter; $n = 7$) ($P < 0.05$ vs. wild-type) compared with that in wild-type mice (10.2 ± 2.5 per square millimeter; $n = 7$) 7 days after UUO. Furthermore, the infiltration of CCR2⁺/Coll⁺ was significantly reduced both in mice treated with anti-CCL21 antibodies (2.9 ± 1.1 per square millimeter; $n = 7$) ($P < 0.05$ vs. wild-type) and in CCR7-null mice (3.4 ± 0.9 per square millimeter; $n = 7$) ($P < 0.05$ vs. wild-type) compared with that in wild-type mice (5.6 ± 1.3 per square millimeter; $n = 7$) 7 days after UUO, whereas there was no difference in the number of CXCR4⁺/Coll⁺ between wild-type mice (8.4 ± 2.3 per square millimeter; $n = 7$), anti-CCL21 antibody-treated mice (9.3 ± 1.7 per square millimeter; $n = 7$), and CCR7-null mice (8.6 ± 3.1 per square millimeter; $n = 7$).

Detection of CCL21-Positive HEV-Like Vessels in Fibrotic Kidney. RT-PCR was performed to determine the renal expression of CCL21 during fibrogenesis. The expression of CCL21 mRNA in diseased kidneys was up-regulated with the progression of fibrosis in wild-type mice after ureteral ligation (Fig. 4a). Furthermore, dual immunostainings were performed to determine the CCL21 expression by HEV-like vessels in diseased kidneys. MECA79 antibody was used immunohistochemically to detect HEV-like vessels in the kidney, because the MECA79-reactive antigen is closely associated with the carbohydrate ligands for L-selectin, which are expressed on HEVs in lymphoid tissues and at sites of chronic inflammation (25). In UUO-treated wild-type mice, CCL21 protein colocalized with MECA79-positive vessels in the corticomedullary regions on day 7 (Fig. 4b-d). The increase in the number of CCL21 and MECA79 dual-positive vessels correlated with the progression of fibrosis after ureteral ligation, reaching a peak on day 7 [7.5 ± 1.1 /all fields on day 7 ($n = 7$) ($P < 0.05$) vs. 0.3 ± 0.2 /all fields on day 0 ($n = 7$)].

Progressive organ fibrosis is pathologically characterized by the presence of infiltrating macrophages and accumulation of extracellular matrix, including Coll I (1). Currently, macrophages are thought to be involved in the development of fibrosis by secreting various cytokines and growth factors including TGF- β_1 (34). Furthermore, recent studies reported that the CCL2/CCR2 signaling pathway is involved in the progression of fibrosis through the recruitment and activation of macrophages in various fibrotic diseases (9, 35–40). CCL2 is reported to be produced by tubular epithelial cells and infiltrating cells in fibrotic kidneys (37). Recently, the expression of CCL2 mRNA was shown to be enhanced in fibrocytes under fibrotic circumstances (11). In addition, the current study demonstrated that renal expression of CCL2 mRNA and the infiltration of F4/80-positive macrophages as well as CCR7-expressing fibrocytes were significantly reduced in mice treated with anti-CCL21 antibodies and in CCR7-null mice after ureteral ligation compared with that in UUO-treated wild-type mice. Our previous reports demonstrated that monocytes/macrophages also contribute to renal fibrosis because the blockade of CCL2/CCR2 signaling resulted in a 30% reduction of renal fibrosis after ureteral ligation (9, 39). In contrast, fibrosis and infiltration of fibrocytes in the kidneys were reduced up to 50% by the inhibition of CCL21/CCR7 signaling in this study. Taken together, these findings suggest that CCR7-expressing fibrocytes are involved in the pathogenesis of fibrosis not only by secreting collagen but also by regulating the infiltration and activation of macrophages through CCL2 production (Fig. 5).

To date, participants involved in the pathogenesis of renal fibrosis have been considered resident fibroblasts, EMT-derived fibroblasts/myofibroblasts, and monocytes/macrophages (6–9). TGF- β_1 is a well characterized inducer of EMT in renal tubular epithelial cells (7), whereas bone morphogenic protein 7 counteracts TGF- β_1 -induced EMT, resulting in improvement of renal fibrosis and renal function in experimental progressive renal diseases (7, 41). Recently, fibrocytes have been demonstrated to be capable of producing TGF- β_1 under fibrotic conditions (11). Therefore, it is possible that fibrocytes regulate EMT through the production of TGF- β_1 (Fig. 5). In addition, a recent report has demonstrated that 36% of renal fibroblasts found in a UUO model were derived from EMT and that 15% were derived from CD34-negative fibroblasts in bone marrow (8). However, fibrocytes detected in this study were positive for leukocyte markers, such as CD34 and CD45; therefore, it is suggested that the origin of fibrocytes may be different from that of CD34-negative fibroblasts. Collectively, fibroblasts derived from EMT and CD34-negative fibroblasts in bone marrow, as well as circulating fibrocytes, may be involved in organ fibrosis. Further investigations are needed to elucidate the origin and mechanisms of differentiation of precursor cells to fibrocytes.

In summary, these findings suggest that CCR7-positive fibrocytes infiltrate the kidney via CCL21-positive HEV-like vessels, thereby contributing to the pathogenesis of renal fibrosis. Regulating the recruitment and activation of fibrocytes may provide a therapeutic approach to combating organ fibrosis.

Materials and Methods

Details are presented in *Supporting Materials and Methods*, which is published as supporting information on the PNAS web site. In

brief, inbred male BALB/c mice, aged 8 wk, were obtained from Charles River Japan (Atsugi, Kanagawa, Japan). CCR7-null mice, aged 8 wk, were also used (42).

All procedures used in the animal experiments complied with the standards set out in the Guidelines for the Care and Use of Laboratory Animals of the Takara-machi campus of Kanazawa University. Unilateral ureteral ligation was performed as previously described (5). To evaluate the impact of CCL21/CCR7 signaling on renal fibrosis as well as infiltrates in diseased kidneys, 600 μ g of rabbit anti-CCL21 polyclonal antibodies (22) in 0.6 ml of normal saline or preimmunized rabbit IgG as a negative control was administered by tail vein 1 h before ureteral ligation. This antibody was obtained by immunizing 3-kg New Zealand White rabbits with 100–200 μ g of recombinant murine CCL21 as previously described (22). The mean interstitial fibrotic area, expressed as blue on Mallory–Azan staining, was determined from the whole area of cortex and outer medulla in the individual complete sagittal kidney section and is expressed as the percentage per square millimeter of the field using Mac Scope version 6.02 (Mitani Shoji, Fukui, Japan).

Fibrocytes were identified in tissue samples by double immunohistochemistry using specific antibodies against CD45 (Santa Cruz Biotechnology, Santa Cruz, CA) or CD34 (BD Pharmingen, San Diego, CA) and Coll I (Chemicon International, Temecula, CA) as previously described (12). Photoshop (Adobe Systems, San Jose, CA) was used for image handling, and three-color channels were handled separately. A preparation of isolated renal cells, including renal resident cells and infiltrated cells, was obtained from normal kidneys, obstructed kidneys, and contralateral kidneys 7 days after UUO in wild-type mice (5). After lysis of erythrocytes with FACS lysing solution (Becton Dickinson, San Jose, CA), cells were stained with FITC-labeled goat anti-mouse CCR2 polyclonal antibodies (Santa Cruz Biotechnology), PerCP-Cy5.5-conjugated rat anti-mouse CXCR4 monoclonal antibody (BD Pharmingen), allophycocyanin-conjugated rat anti-mouse CCR7 monoclonal antibody (BioLegend, San Diego, CA), and R-phycoerythrin-labeled rabbit anti-mouse Coll I polyclonal antibodies (Chemicon International), and then analyzed on a FACSCalibur flow cytometer using CELLQuest software (Becton Dickinson). Cells incubated with irrelevant isotype-matched antibodies (BD Pharmingen) and unstained cells were used as controls. The cutoffs were set according to the findings in controls.

The expression of COL1A1, TGF- β_1 , and CCL2 in the whole kidneys was determined by quantitative real-time RT-PCR using the ABI Prism 7900HT Sequence Detection System (Applied Biosystems, Foster City, CA). Transcripts of CCL21 in diseased kidneys were also estimated by semiquantitative RT-PCR. Statistical analyses were performed by using the Wilcoxon rank-sum test, the Kruskal–Wallis test, and ANOVA.

We thank Drs. Yuko Ishida and Toshikazu Kondo (Wakayama Medical University, Wakayama, Japan) for technical advice in the measurement of hydroxyproline contents and Dr. Joost J. Oppenheim (National Cancer Institute) for critical review of the manuscript. T.W. is the recipient of a grant-in-aid from the Ministry of Education, Science, Sports, and Culture in Japan. This work was supported in part by a grant-in-aid from the Ministry of Health, Labor, and Welfare of Japan.

1. Wada T, Razzaque MS, Matsushima K, Taguchi T, Yokoyama H (2004) in *Fibrogenesis: Cellular and Molecular Basis*, ed Razzaque MS (Landes Bioscience Eureka, Washington, DC), pp 9–26.
2. Bohle A, Muller GA, Wehrmann M, Mackensen-Haen S, Xiao JC (1996) *Kidney Int Suppl* 49:S2–S9.
3. Risdon RA, Sloper JC, de Wardener HE (1968) *Lancet* 2:363–366.
4. Nath KA (1998) *Kidney Int* 54:992–994.
5. Vielhauer V, Anders HJ, Mack M, Cihak J, Strutz F, Stangassinger M, Luckow B, Grone HJ, Schlöndorff D (2001) *J Am Soc Nephrol* 12:1173–1187.
6. Strutz F, Zeisberg M, Ziyadeh FN, Yang CQ, Kalluri R, Muller GA, Neilson EG (2002) *Kidney Int* 61:1714–1728.
7. Zeisberg M, Hanai J, Sugimoto H, Mammoto T, Charytan D, Strutz F, Kalluri R (2003) *Nat Med* 9:964–968.
8. Iwano M, Plieth D, Danoff TM, Xue C, Okada H, Neilson EG (2002) *J Clin Invest* 110:341–350.
9. Kitagawa K, Wada T, Furuichi K, Hashimoto H, Ishiwata Y, Asano M, Takeya M, Kuziel WA, Matsushima K, Mukaida N, Yokoyama H (2004) *Am J Pathol* 165:237–246.
10. Bucala R, Spiegel LA, Chesney J, Hogan M, Cerami A (1994) *Mol Med* 1:71–81.

11. Chesney J, Metz C, Stavitsky AB, Bacher M, Bucala R (1998) *J Immunol* 160:419–425.
12. Moore BB, Kolodnick JE, Thannickal VJ, Cooke K, Moore TA, Hogaboam C, Wilke CA, Toews GB (2005) *Am J Pathol* 166:675–684.
13. Phillips RJ, Burdick MD, Hong K, Lutz MA, Murray LA, Xue YY, Belperio JA, Keane MP, Strieter RM (2004) *J Clin Invest* 114:438–446.
14. Schmidt M, Sun G, Stacey MA, Mori L, Mattoli S (2003) *J Immunol* 171:380–389.
15. Abe R, Donnelly SC, Peng T, Bucala R, Metz CN (2001) *J Immunol* 166:7556–7562.
16. Hauser C, Kaya G, Chizzolini C (2004) *Dermatology* 209:50–52.
17. Yang L, Scott PG, Giuffre J, Shankowski HA, Ghahary A, Tredget EE (2002) *Lab Invest* 82:1183–1192.
18. Okon K, Szumera A, Kuzniewski M (2003) *Am J Nephrol* 23:409–414.
19. Campbell JJ, Bowman EP, Murphy K, Youngman KR, Siani MA, Thompson DA, Wu L, Zlotnik A, Butcher EC (1998) *J Cell Biol* 141:1053–1059.
20. Gunn MD, Tangemann DK, Tam C, Cyster JG, Rosen SD, Williams LT (1998) *Proc Natl Acad Sci USA* 95:258–263.
21. Ogata M, Zang Y, Wang Y, Itakura M, Zang YY, Harada A, Hashimoto S, Matsushima K (1999) *Blood* 93:3225–3232.
22. Itakura M, Tokuda A, Kimura H, Nagai S, Yoneyama H, Onai N, Ishikawa S, Kuriyama T, Matsushima K (2001) *J Immunol* 166:2071–2079.
23. Wright F (1982) *Semin Nephrol* 2:5–16.
24. Klahr S (1983) *Kidney Int* 23:414–426.
25. Michie SA, Streeter PR, Bolt PA, Butcher EC, Picker LJ (1993) *Am J Pathol* 143:1688–1698.
26. Kraal G, Mebius RE (1997) *Adv Immunol* 65:347–395.
27. Baekkevold ES, Yamanaka T, Palframan RT, Carlsen HS, Reinhold FP, von Andrian UH, Brandtzaeg P, Haraldsen G (2001) *J Exp Med* 193:1105–1112.
28. Dinther-Janssen ACHM, Pals ST, Scheper R, Breedveld F, Meijer CJLM (1990) *J Rheumatol* 17:11–17.
29. Kabel PJ, Voorbij HAM, Haan-Meulman M, Pals ST, Drexhage HA (1989) *J Clin Endocrinol Metab* 68:744–751.
30. Weninger W, Carlsen HS, Goodarzi M, Moazed F, Crowley MA, Baekkevold ES, Cavanagh LL, von Andrian UH (2003) *J Immunol* 170:4638–4648.
31. Takaeda M, Yokoyama H, Segawa-Takaeda C, Wada T, Kobayashi K (2002) *Am J Nephrol* 22:48–57.
32. Riol-Blanco L, Sanchez-Sanchez N, Torres A, Tejedor A, Narumiya S, Corbi AL, Sanchez-Mateos P, Rodriguez-Fernandez JL (2005) *J Immunol* 174:4070–4080.
33. Sato M, Shegogue D, Gore EA, Smith EA, McDermott PJ, Trojanowska M (2002) *J Invest Dermatol* 118:704–711.
34. Border WA, Noble NA (1994) *N Engl J Med* 331:1286–1292.
35. Suga M, Iyonaga K, Ichiyasu H, Saita N, Yamasaki H, Ando M (1999) *Eur Respir J* 14:376–382.
36. Lehmann MH, Kuhnert H, Muller S, Sigusch HH (1998) *Cytokine* 10:739–746.
37. Wada T, Furuichi K, Segawa C, Shimizu M, Sakai N, Takeda S, Takasawa K, Kida H, Kobayashi K, Mukaida N, et al. (1999) *Kidney Int* 56:995–1003.
38. Moore BB, Paine R, III, Christensen PJ, Moore TA, Sitterding S, Ngan R, Wilke CA, Kuziel WA, Toews GB (2001) *J Immunol* 167:4368–4377.
39. Wada T, Furuichi K, Sakai N, Iwata Y, Kitagawa K, Ishida Y, Kondo T, Hashimoto H, Ishiwata Y, Mukaida N, et al. (2004) *J Am Soc Nephrol* 15:940–948.
40. Wada T, Yokoyama H, Furuichi K, Kobayashi K, Harada K, Naruto M, Su SB, Akiyama M, Mukaida N, Matsushima K (1996) *FASEB J* 12:1418–1425.
41. Hruska KA, Guo G, Wozniak M, Martin D, Miller S, Liapis H, Loveday K, Klahr S, Sampath TK, Morrissey J (2000) *Am J Physiol* 280:F130–F143.
42. Forster R, Schubel A, Breitfeld D, Kremmer E, Muller IR, Wolf E, Lipp M (1999) *Cell* 99:23–33.